sustainability

MDPI

Article

Development of High-Strength Geopolymer Concrete Incorporating High-Volume Copper Slag and Micro Silica

Nagarajan Arunachelam [1], Jeyaprakash Maheswaran [2], Maheswaran Chellapandian [1,*], Gunasekaran Murali [3,*] and Nikolai Ivanovich Vatin [3]

[1] Department of Civil Engineering, Mepco Schlenk Engineering College, Sivakasi 626005, India; arunachelam.n@mepcoeng.ac.in
[2] Department of Civil Engineering, St. Xaviers Catholic College of Engineering, Nagercoil 629004, India; drjmaheswaran@gmail.com
[3] Peter the Great St. Petersburg Polytechnic University, 195251 Saint Petersburg, Russia; vatin@mail.ru
* Correspondence: chellapandian@mepcoeng.ac.in (M.C.); murali_22984@yahoo.com (G.M.)

Abstract: The present work investigates the mechanical and chemical characteristics and durability of high-strength geopolymer concrete (HSGPC) developed using high-volume copper slag and micro silica. The objective of the study was to explore the feasibility of deploying high-volume copper slag as a replacement for river sand in the fabrication of high-strength geopolymer concrete. In total, 11 different trials were cast by varying copper slag up to 100% as a potential alternative for the river sand. The mixture of alkaline activators for the preparation of the geopolymer concrete (GPC), such as sodium silicate (Na_2SiO_3) and sodium hydroxide (12 M NaOH), was used in the ratio 2.5:1. The optimum mix was selected from different copper slag dosages based on the characteristics of the HSGPC, such as mechanical strength and workability. For the selected optimized mix, micro silica was added up to 5% by volume of the binder (i.e., 1%, 2%, 3%, 4% and 5%) to improve the particle packing density of the developed HSGPC mix which in turn further enhances the strength and durability properties. Two different curing methods, including (a) ambient curing and (b) steam curing at 80 °C, were deployed for achieving the polymerization reaction (i.e., the formation of Na-Al-Si-H gel). Experimental outcomes reveal a maximum compressive strength of 79.0 MPa when 2% micro silica was added to the optimized GPC mix. In addition to the mechanical tests, the quality of the developed HSGPC was assessed using the ultrasonic pulse velocity (UPV) tests, water-absorption tests, sorptivity tests and microstructural analyses.

Keywords: high-strength geopolymer concrete; copper slag; micro silica; ambient curing; steam curing

check for updates

Citation: Arunachelam, N.; Maheswaran, J.; Chellapandian, M.; Murali, G.; Vatin, N.I. Development of High-Strength Geopolymer Concrete Incorporating High-Volume Copper Slag and Micro Silica. *Sustainability* **2022**, *14*, 7601. https://doi.org/10.3390/su14137601

Academic Editor: Antonio Caggiano

Received: 18 May 2022
Accepted: 18 June 2022
Published: 22 June 2022

Publisher's Note: MDPI stays neutral with regard to jurisdictional claims in published maps and institutional affiliations.

Copyright: © 2022 by the authors. Licensee MDPI, Basel, Switzerland. This article is an open access article distributed under the terms and conditions of the Creative Commons Attribution (CC BY) license (https://creativecommons.org/licenses/by/4.0/).

1. Introduction

In developing countries such as India, the rapid growth in the infrastructure sector leads to a large demand in the production of concrete. It is reported from a recent survey that the global production of concrete per annum is more than 10 million tons which is a significantly large number [1]. Moreover, Portland cement, which is a major ingredient of concrete, requires intensive energy for its production and utilizes a huge amount of raw materials. In addition to the energy consumption, the cement production emits tons of CO_2 into the atmosphere leading to a significant increase in the greenhouse gases present in the atmosphere [2]. As per a recent survey, the production of Portland cement accounts for a total CO_2 emission of 2.3 giga tonne, out of which 1.4 giga tone is emitted due to the clinker production [2]. Hence, a number of alternatives that possess excellent cementitious properties are being researched around the world, which could act as a potential replacement for cement. Also, the current major problem faced by the manufacturing industries is the disposal of their wastes or by-products. In India, coal/lignite-based thermal power plants act as the backbone of the country power generation. According to reports, more than 233 million tons of fly ash were created by thermal power plants across India [3]. Hence,

a number of previous works have investigated the effect of the complete replacement of cement with fly ash in the production of concrete [4–6].

Geopolymer concrete is one such alternate for conventional concrete and is synthesized through the use of an alumino-silicate source material obtained from natural origin or industrial by-products [7–10]. In GPC, the conventional binding material is totally replaced using low-calcium fly ash. Geopolymer concrete is produced by the reaction of the source material rich in alumino-silicates in a high-alkaline environment. During this reaction, the free silica (SiO_2) and tetrahedral units of alumina (AlO_4) are dissolved and released in the mix [11–13]. Compared to the cement-based concrete, geopolymers require only three-fifths the energy for the production and emit only 80–90% less carbon dioxide [14]. Moreover, GPC possesses excellent temperature resistance characteristics and can withstand up to 1200 °C, enduring about 50 kw/m^2 fire exposures without sudden degradation in the mechanical properties [14]. Fly ash is one of the most widely used industrial by-products for the mass manufacturing of GPC because it has a sufficient amount of reactive silica and alumina [15–20]. The effect of temperature on the GPC made using different levels of fly ash and kaolinite is investigated in a number of previous works [21–25]. Although fly ash has been completely used as a replacement for cement, the low calcium content and the low heat of the hydration inhibits the practical application of GPC because it requires elevated temperatures to achieve polymerization. Hence, the total content of fly ash in GPC has been replaced using ground-granulated blast-furnace slag up to 30% to achieve the polymerization process even in the ambient-curing conditions [26].

Silica fume (SF), which is a by-product from the smelting process of silicon and the ferrosilicon industry, can be obtained during the carbo-thermic reduction of highly pure quartz. It is characterized by the presence of a micro sphere of non-crystalline silica, having a mean size of 0.1–0.3 µm with an excessive surface area [27–29]. Hence, the addition of micro silica as an alternate cementing material enhances the load and durability resistance of concrete due to their better pozzolanic reactivity. Hence, the mechanical properties of the developed mix are improved by offering the active SiO_2 for the geopolymerization process and the structure is made denser [30–32]. Das et al. [29] researched the microstructural and strength characteristics of micro silica and lime-based GPC under ambient-curing conditions. They justified that the replacement of fly ash with lime resulted in reduced workability and initial setting time. However, the compressive strength and microstructural properties of concrete were enhanced when used in combination with the silica fume. Adak et al. [33] studied the behavior of GPC manufactured using the nano-silica. They showed that the nano-silica addition helped in enhancing the polymerization of geopolymers even in ambient conditions. Okoye et al. [34] studied the durability characteristics of geopolymer concrete made with micro silica and low-calcium fly ash. They found that the presence of 20% silica fume showed no real signs of deterioration under 90 days of 2% H_2SO_4 solution and 5% NaCl treatment when compared to the conventional cement-based concrete.

Aggregates occupy more than 70% of the total volume in concrete. Due to the rapid development in the economy and the ensuing rise of building activities, a great hike in the deployment of river sand can be witnessed in developing countries such as India [35]. River sand collected from the riverbed and open pits could result in significant land degradation, disturbance to the water table, ecological imbalance and damage to the land-use patterns [36]. Because most of the natural sand deposits are being depleted due to the continuous exploitation, the use of an alternative fine aggregate in concrete is gaining attention. Previously, various authors have investigated the effect on concrete of the partial replacement of different materials, such as crushed rock particles, pond ash, manufactured sand, washed soil, quarry dust, pond ash, copper slag, powdered brick, offshore sand, construction demolition waste and powdered glass [37–41]. Copper slag is also the industrial by-product obtained during the matte-smelting process of raw copper. From the available reports, it can be noticed that more than 2.2 tons of copper slag is generated for every ton of copper production which accounts for a global copper slag production of 51.7 million tons [42]. The mineralogical composition and morphology of

the slag show that it can be used in the construction industry as a potential replacement for river sand [43–48]. Palani et al. [49] studied the compression load resistance and durability properties of copper slag-based high-strength concrete (HSC). The authors have substituted copper slag for river sand in steps of 10 to 100%. They found that the copper slag replacement did not show any detrimental effects on the durability and mechanical strength of high-strength concrete. Al-Jabri et al. [50] studied the effectiveness of the copper slag addition as a substitute for river sand. They found that the use of copper slag up to 50% helped in effectively increasing the strength and durability without any detrimental effects. Sharma and Khan [51] investigated the consequence of the copper slag addition on the overall mechanical and microstructural behavior of self-compacting concrete (SCC). In addition, silica fume and low-calcium fly ash were used as the supplementary cementitious material. They observed a good enhancement in the tensile and compression resistance when compared to the conventional concrete mix. Moreover, the microstructural analyses using a scanning electron microscope (SEM) showed the development of uniformly distributed and compact C-S-H gel due to the copper slag replacement. Sivasakthi et al. [52] studied the use of copper slag on fly ash-based geopolymer mortar and reported that the suitability of copper slag as the aggregate is possible in a sustainable way for high-temperature applications, and it possesses better thermal stability even at 1000 °C without spalling. At this temperature, thermal conductivity was found to be 0.6 W/m with a compressive strength of 33 MPa. In recent decades, there is great pursuit against the immobilization of heavy metals using geopolymers, and this was due to the excellent characteristic or performance of the geopolymer. The monolithic products of the geopolymer help increase immobilization efficiency for heavy metals, such as Lead, Arsenic, Boron, Caesium and strontium; radioactive waste products such as radium and uranium are also immobilized with a higher success rate [53–60]. Metallic elements can also be trapped in the geopolymer binder in the form of precipitated hydroxides, which leads to a higher resistance to leaching [61].

Though a number of previous works have focused on the development of eco-friendly geopolymer concrete, only limited studies are available on the ambient-cured geopolymer concrete. In general, no research works are available on the deployment of micro silica for the production of high-volume copper slag-based geopolymer concrete. Moreover, two different curing methods, ambient curing and steam curing, are explored to understand the extent of the polymerization process at different time intervals. The overall objective is to examine the microstructural, mechanical and durability characteristics of high-volume copper slag-based high-strength geopolymer concrete prepared with different doses of micro silica. The following are the distinct contributions made through this work.

(a) Developing a sustainable high-strength geopolymer concrete (HSGPC) with high-volume copper slag as a replacement for conventional river sand.

(b) Quantifying the need for the micro silica addition on the strength, durability and microstructural characteristics of high-strength geopolymer concrete (HSGPPC) with optimized copper slag.

(c) Understanding the performance of different curing methods such as steam curing and ambient curing on the overall properties of the HSGPC prepared using micro silica and copper slag.

2. Experimental Program

2.1. Class-F Fly Ash

Low-calcium-based Class-F fly ash was used as a main binder for the preparation of GPC, and it was procured from the Tuticorin thermal power plant. The density and specific gravity of fly ash used was determined as 1.6 g/cm^3 and 2.03. The chemical composition of fly ash in this work was obtained from the X-ray florescence (XRF) analysis (Table 1). From Table 1, it can be inferred that the fly ash sample contains high amount of silica (69.6%), alumina (14.8%) and iron (3.3%) which satisfies the ASTM guidelines for Class-F category [62]. The particle size distribution curve of the fly ash was obtained from the laser

diffraction scattering method (Shimadzu SALD-2300), and the mean diameter of the fly ash particle was found to be 11.928 µm with a coefficient of variation of 0.7 µm.

Table 1. Chemical composition of materials.

Components	Fly Ash	Copper Slag
Silica (SiO_2)	69.583	44.382
Alumina (Al_2O_3)	14.825	3.169
Reference Iron oxide (Fe_2O_3)	3.313	42.942
Calcium oxide (CaO)	4.510	2.356
Magnesium oxide (MgO)	1.620	4.251
Sodium oxide (Na_2O)	4.723	0.030
Sulphur tri-oxide (SO_3)	0.497	2.573
Loss of Ignition	0.929	0.297

Microstructure of the samples are studied through the VEGA3 TESCAN scanning electron microscope (SEM) analyses. Results reveal that the particles present are mostly in spherical shape except for a few irregularly shaped particles (Figure 1a). The SEM images also revealed the presence of a glassy phase in fly ash which could enhance the workability of GPC because of the ease in mixing and flow. In order to study the crystalline structure of fly ash, the diffraction pattern for fly ash was found using the X-ray Diffractometer (XRD) and the result is presented in Figure 2a. Results from the XRD analyses revealed the presence of crystalline phase in fly ash through a number of sharp peaks in the XRD graphs. In addition to the sharp peaks, few humps were also found which indicates the amorphous phase in fly ash. Comparing the peaks observed, a prominent diffuse peak can be found at 26° (2θ), confirming the crystalline stages of quartz and mullite in the fly ash [43]. In addition, the silica and alumina are identified to be in amorphous glass phase in the region between 14° and 30° as a broad diffraction hump.

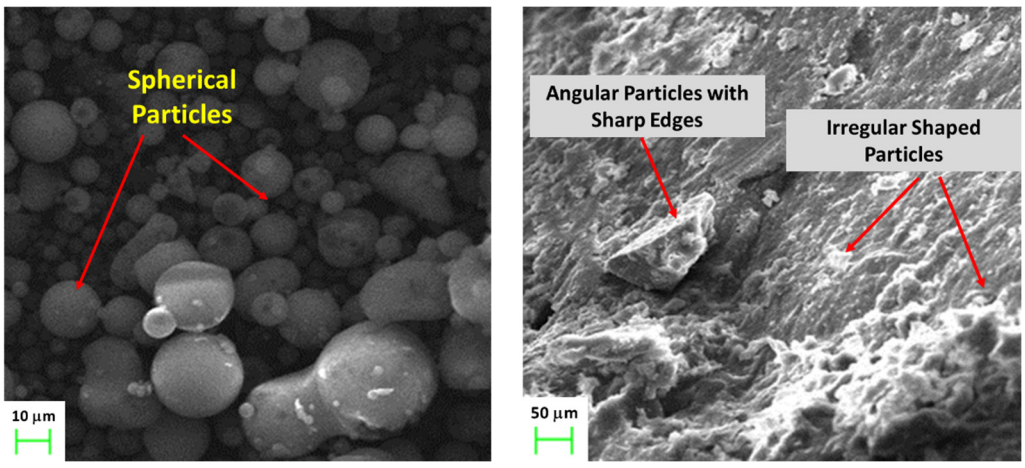
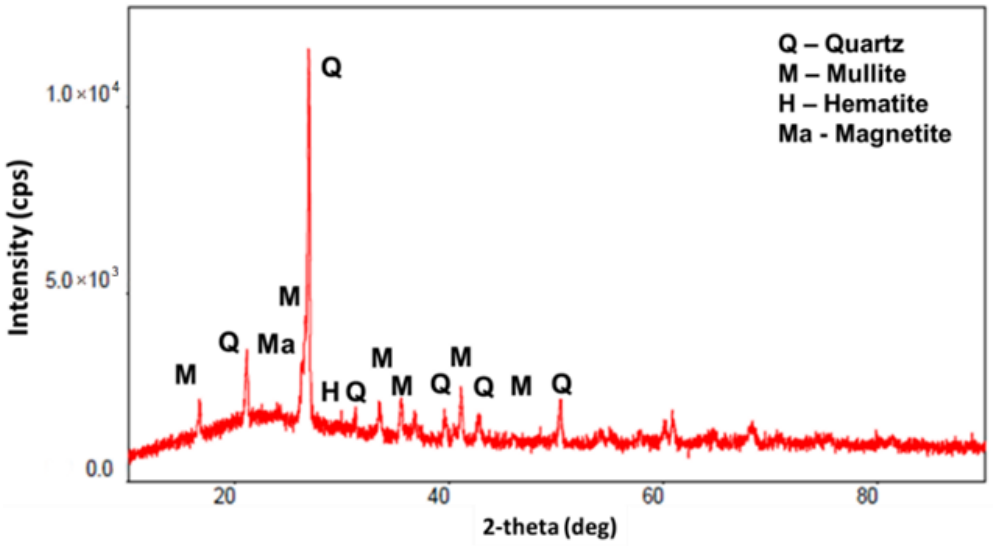


Figure 1. Microstructure images of fly ash and copper slag. (**a**) Fly ash; (**b**) copper slag.

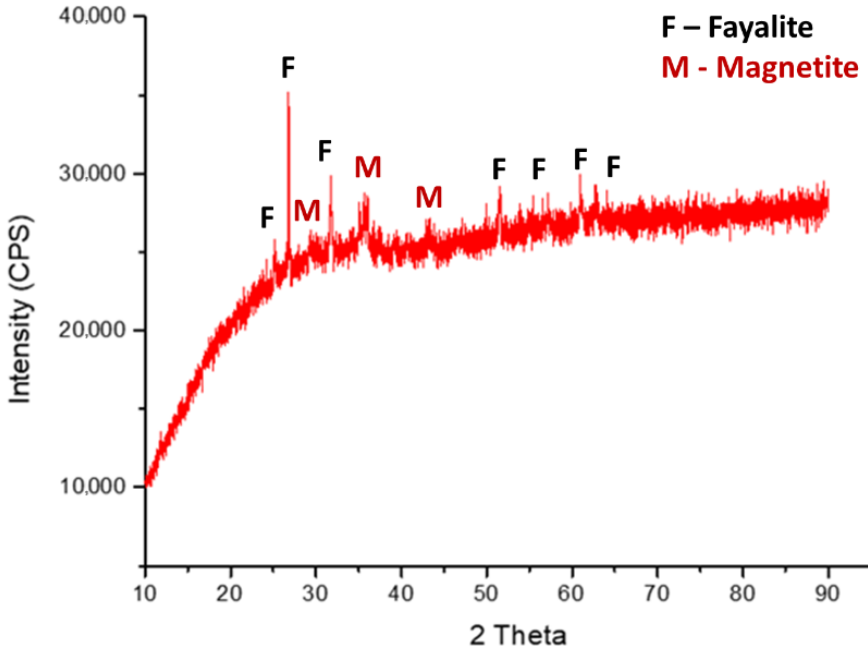
2.2. Copper Slag

Copper slag is a glassy, granular substance, black in color in physical appearance, and it was obtained from Sterlite Industries (India) Ltd., Thoothukudi, Tamil Nadu, India. The material properties of copper slag such as water absorption and density were found to be 0.23% and 2.86 g/cm^3, respectively. It is worth mentioning that the value of specific gravity was 3.58 due to the presence of high iron content as observed from XRF analysis shown in Table 1. Figure 1b depicts the SEM analysis of copper slag, highlighting the presence of large number of angular and irregularly shaped particles. XRD analyses of copper slag were performed at a step size of 0.1°. Results reveal the amorphous nature with no distinct

peaks (Figure 2b). A few ferrous peaks such as fayalite ($2FeO{\cdot}SiO_2$) and magnetite (Fe_3O_4) can be observed, and the same has been reported in previous studies [63,64].



(**a**)



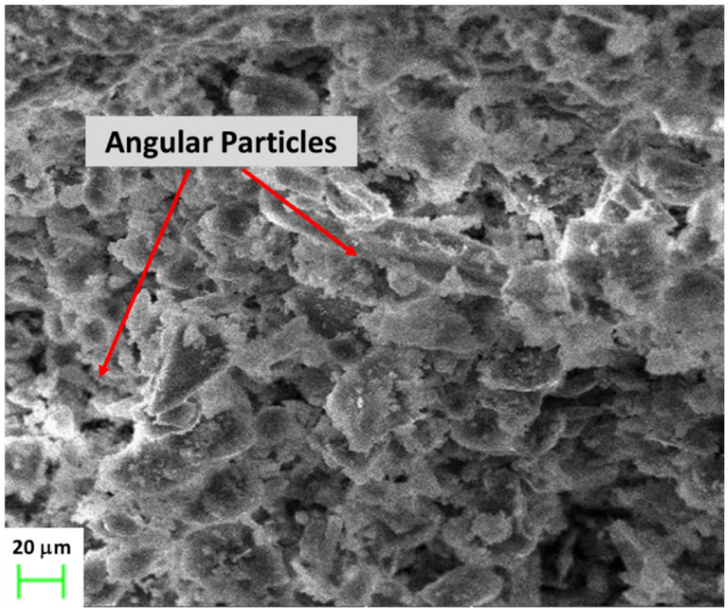
(**b**)

Figure 2. Microstructure characterization of copper slag. (**a**) Fly ash; (**b**) copper slag.

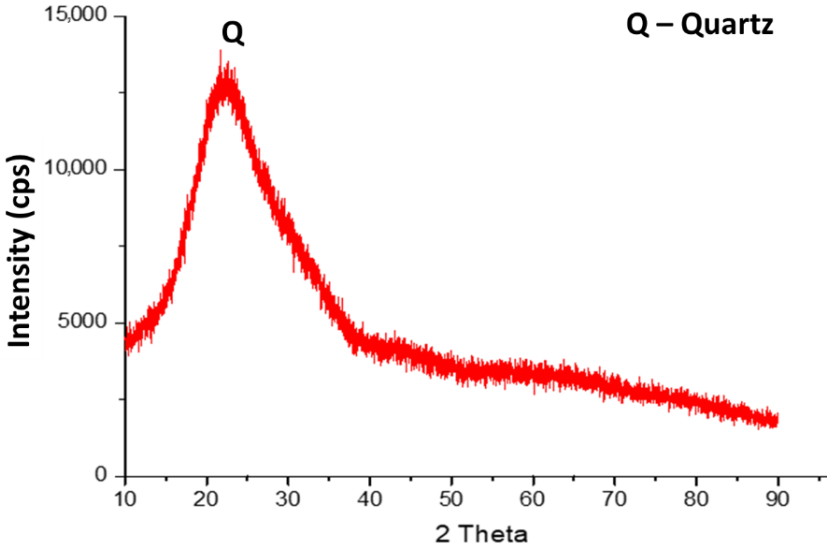
2.3. Silica Fume

Micro silica or silica fume is a supplementary cementitious material used as an artificial pozzolanic admixture. The average diameter of micro silica is 100 times smaller when compared to the Portland cement, showing its extreme fine characteristics [34]. Moreover, the use of micro silica in concrete could initiate a rapid reaction and thereby help in achieving high early strength. Hence, it can be mentioned that the efficiency of micro silica is 3–5 times higher when compared to the conventional Portland cement. Moreover, the density of silica fume was found to be 1.8 g/cm^3. Figure 3a shows the SEM image of micro silica or silica fume. From the microstructure analyses, it can be found that the silica fume contains a large number of angular and irregular particles. From the XRD results of silica

fume, it is clear that micro silica is generally amorphous in nature which can be attributed to the surface tension in the phase transition and rapid condensation of volatile SiO_2 and Si gases (Figure 3b). But a few sharp diffraction peaks at approximately $2\theta = 25^\circ$ are due to the presence of quartz [65–67].



(**a**)



(**b**)

Figure 3. Microstructure image of micro silica (**a**) SEM and (**b**) XRD.

2.4. River Sand

Sand obtained from the local riverbed confirming the Zone-II category as per IS 383-2016 [68] was used as fine aggregate. Figure 4 shows the particle-size distribution graph for river sand. The sand particles follow a smooth "s-shaped" distribution curve showing their well-graded nature. Also, the values of fineness modulus and density were experimentally determined as 2.57 and 2.52 g/cm^3, respectively. From the XRF analyses, the chemical composition of river sand was analyzed. XRF analyses confirmed the presence of more than 95% silica (SiO_2) with the other oxide compounds in comparatively negligible percentage. The particle-size distribution curve is presented in Figure 4.

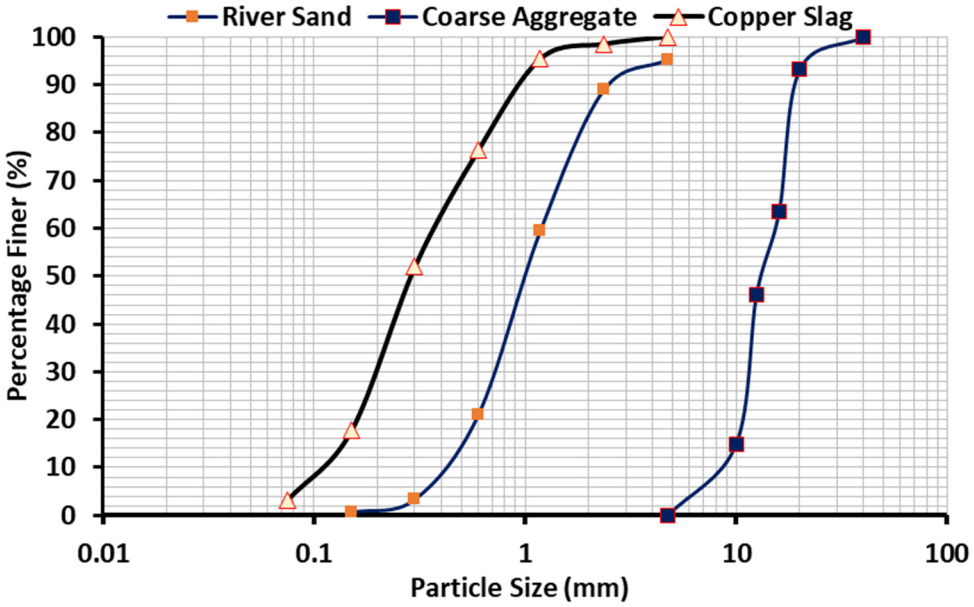


Figure 4. Particle-size distribution comparison for C.A., copper slag and river sand.

2.5. Coarse Aggregate

Blended aggregates (size: 20 and 10 mm) procured from the local quarry were used in this work. The density of coarse aggregate was found to be 2.74 g/cm^3. Figure 4 depicts the particle-size distribution graph of the coarse aggregate compared with the river sand and copper slag. From Figure 4, it is clear that the coarse aggregates are also well-graded and show a smooth "S-curve" pattern in the particle-size distribution diagram.

2.6. Alkaline Activators

In this study, sodium silicate (Na_2SiO_3) and sodium hydroxide (NaOH) were used as the alkaline solutions for the preparation of GPC. The use of NaOH and Na_2SiO_3 helps the gel formation through the dissolution of alumina and silica from the Si-Al source materials (fly ash, copper slag) to form hydration product. In this work, NaOH flakes were procured and dissolved in the ionized water to achieve the required molarity [69]. In this work, sodium hydroxide solution with 12 M was prepared. The following are the chemical configuration of sodium silicate solution: SiO_2—29.6, Na_2O—14.8% and H_2O—55.6%. Higher levels of NaOH molarity were not preferred due to the difficulties in mixing and handling the prepared GPC mix. Sodium silicate was procured in the liquid form and used for the mix preparation. The ratio of NaOH and Na_2SiO_3 was kept as 1:2.5 [70,71].

3. Production of High-Strength Copper Slag-Based GPC with Micro Silica

Table 2 presents the details of the mix design used for the fabrication of the high-strength copper slag-based geopolymer concrete where the dosage of copper slag was incremented in levels of 10%. The mix design for the control specimen with no copper slag was performed as per the trial-and-error procedure. For achieving a target compressive strength of 40 MPa, a number of trials for the control GPC mix were performed by varying the alkaline activator ratio and binder ratio. After fixing the dosage for the control specimen, all the parameters, such as ratio of NaOH and Na_2SiO_3 (1:2.5), quantity of fly ash (480 kg/m^3) and coarse aggregate (1139 kg/m^3), were kept constant. The SiO_2/Na_2O mole ratio of the sodium silicate solution was maintained as 2.0. Then, 11 trial mixes were cast by varying the quantity of copper slag to 100% to determine and finalize the optimum mix. From the results of the 11 mixes, the optimized mix proportion was selected and added with different proportions of micro silica (1 to 5%) in the stages of 1%. For the preparation of the GPC mix, the sodium hydroxide (NaOH) solution prepared for the 12 M concentration is blended with the sodium silicate solution to form the alkaline activator. In order to enhance

the workability of the developed GPC mix, sulphonated naphthalene formaldehyde (SNF) solution was added, 4% of the mass of the binding material used. During the preparation of the GPC mix with copper slag, the mix was harsh due to the higher viscosity of the alkaline liquid. The addition of extra water during the mixing of the GPC could add a negative impact on the strength. Hence, the dosage of the super-plasticizer is kept constant at 4% for all the mixes. Also, it is worth mentioning that the dosage was finalized from a few previous works which have provided super-plasticizers up to 6% in GPC [72,73].

Table 2. Mix design for the GPC using trial-and-error procedure.

Mix ID	M0	M1	M2	M3	M4	M5	M6	M7	M8	M9	M10
Materials *	0%	10%	20%	30%	40%	50%	60%	70%	80%	90%	100%
Copper Slag *	0	94	188	282	376	470	564	658	752	846	940
River Sand *	613	551	490	429	367	306	245	183	122	61	0
NaOH *	53										
Na_2SiO_3 *	132.5										
Fly ash *	480										
C.A *	1139										

* The units of all the values are in kg/m^3.

For the mixing of the HSGPC, the dry materials of a specified quantity were initially dry-mixed in the pan mixer. Then, the alkaline activator solution and chemical admixture were slowly added to the initial mix until the mixture gets transformed to a workable one. The prepared fresh mix was cast into the standard cube and cylinder molds of size 100 mm, and 100 mm (diameter) × 200 mm (height), respectively. After the casting procedure, the specimens were left for pre-curing for 24 h at room temperature and de-molded. The pre-curing process aids in improving the strength of the developed HSGPC by the dissolution of the alumina and silica present in the fly ash. Moreover, this pre-curing process aids in improving the homogeneity of the geopolymeric material [74,75]. After pre-curing, a set of specimens were transferred to the steam chamber to facilitate the steam-curing process and the remaining ones were left to facilitate the ambient-curing condition. The following are the details of the steam curing provided for the GPC specimens: heating rate—80 °C for 8 h, cooling rate—1 °C per minute and total steam-curing time—24 h.

4. Results and Discussion

The developed GPC mixes were tested for compressive strength at different ages: 3, 7 and 28 days. Then, the optimized mix was selected based on the compressive strength achieved and used for further strength and durability characteristics.

4.1. Tests on Trial Mixes

4.1.1. Workability Test

A slump cone test was carried out to understand the result of the copper slag addition on the workability of the geopolymer concrete. From the results of the slump test, the control geopolymer concrete mix with no copper slag resulted in a slump value of 69 mm (medium slump). Moreover, it can be established that the higher volume of the copper slag addition for the replacement of the river sand shows a drastic reduction in the workability of the geopolymer concrete. Due to the particle shape (angular and irregular) and density, the higher levels of the copper slag replacements resulted in a harsh concrete mix. As per EN206, the slump value in the range 10–40 mm is considered stiff. However, most of the GPC mixes come under the category "plastic" and only a few mixes (M8, M9 and M10) can be classified under stiff or low-workable concrete. Vibrator-based compaction is conducted for achieving a dense compaction in order to ensure better results for low-workable concrete mixes.

The reduction in the slump value is due to the physical characteristics of the material used in the concrete and the amount of copper slag present in the mix. Due to the replace-

ment of the copper slag up to 100%, the density of the concrete increases up to 2632 kg/m^3. The copper slag addition resulted in an increase in density of 9.3% when compared to the conventional GPC without copper slag. When the copper slag was replaced more than 50%, the GPC mix becomes much stiffer and is harder to fill-in and compact in the molds as a result of which the workability was considerably reduced. Also, the workability reduction could also be due to the increase in the density of the GPC mix when the copper slag was added at a higher volume. Moreover, the reduced slump value may be due to the higher viscosity of the alkaline liquid used in the concrete mix, as no additional water is added during the mixing to achieve better compressive strength.

4.1.2. Compressive Strength of HSGPC Trial Mixes

The compression test for the high-strength geopolymer concrete (HSGPC) trial mixes were performed in accordance with the IS 516-1959 [76]. Figure 5 depicts the results obtained for the cubes which are cured at ambient- and steam-curing conditions and further tested at different ages, the 3rd, 7th and 28th day. From Figure 5, a gradual rise in the compressive strength of the HSGPC can be witnessed with an increase in curing time which clearly indicates the continuation of the geopolymerization reaction. The temperature and the curing duration greatly impact the strength development of the geopolymer concrete. In ambient curing, the strength of the concrete increases with the increase in the curing period. Only after 28 days, the ambient-cured GPC specimens attained sufficient compressive strength. However, in the case of the steam-cured specimens, more than 80% of the target compressive strength of the GPC specimen was achieved on the 3rd day. After the 3rd day, the enhancement in the compressive strength was marginal for the steam-cured specimens. Table 3 demonstrates the compressive strength of specimens under ambient and steam curing.

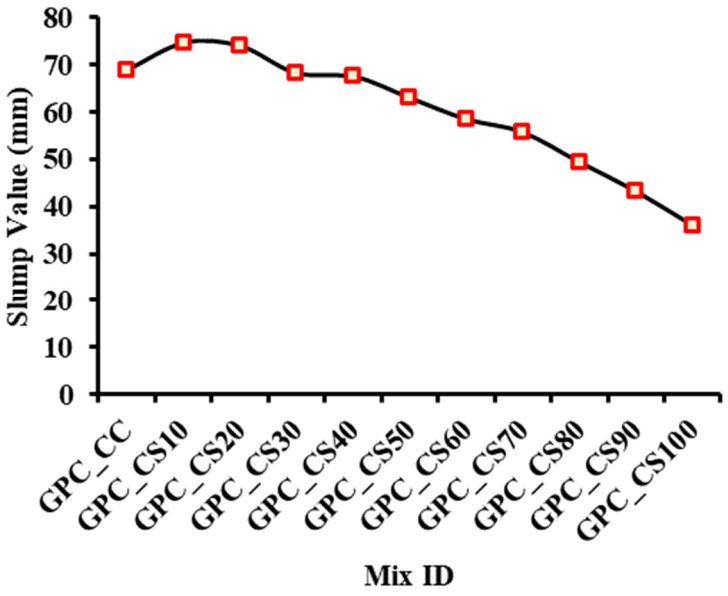


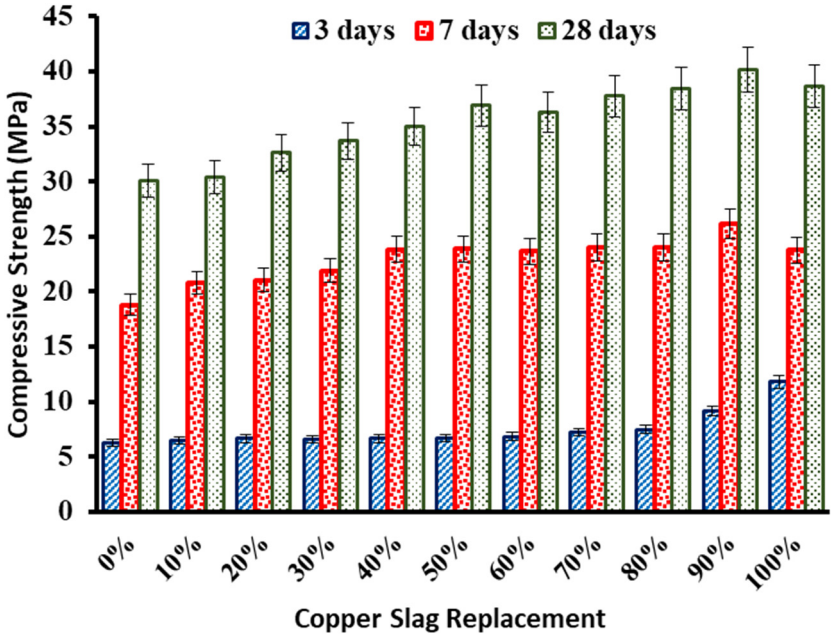
Figure 5. Slump test on GPC trial mixes with different percentage of copper slag.

When compared to the steam-cured specimens, the gain in compressive strength was much slower in the ambient-cured concrete. The strength enhancement of the developed HSGPC is due to the formation of the sodium-alumino-silicate-hydrate (N-A-S-H) gel. However, this development of the N-A-S-H gel consumes a higher time in the case of the ambient-curing conditions. Comparing the different mixes, the GPC specimens with 90% copper slag had the highest value of compressive strength in the case of both the ambient- and steam-curing conditions, respectively.

Table 3. Comparison of results for the trial GPC mixes.

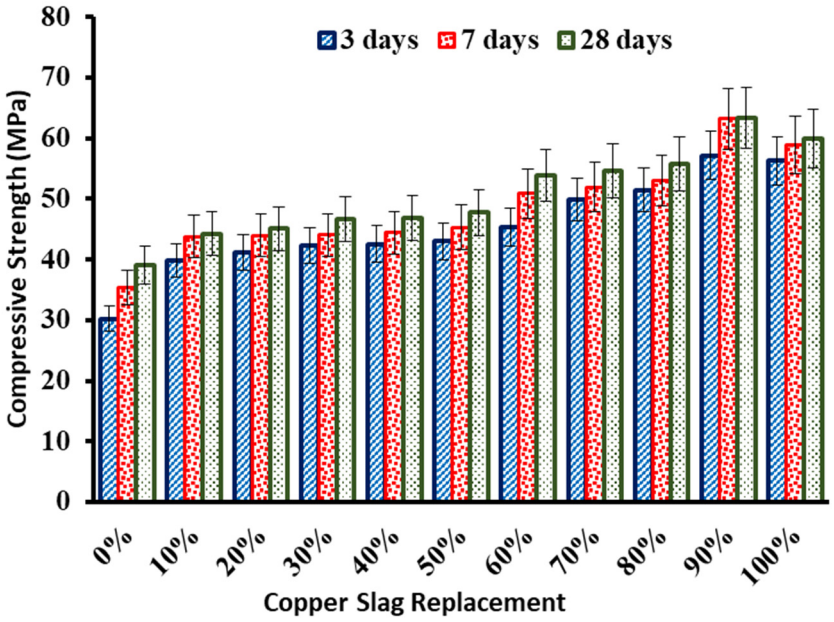
Mix ID	Slump (mm)	Compressive Strength for Ambient-Cured GPC (Mpa)			Compressive Strength for Steam-Cured GPC (Mpa)		
		3 Days	7 Days	28 Days	3 Days	7 Days	28 Days
GPC_CC	69	6.3	18.79	30.08	30.23	35.38	39.08
GPC_CS10	75	6.49	20.77	30.42	39.81	43.75	44.27
GPC_CS20	74	6.64	21.03	32.59	41.15	43.98	45.13
GPC_CS30	68	6.61	21.89	33.68	42.30	44.01	46.67
GPC_CS40	68	6.64	23.81	35.01	42.56	44.4	46.89
GPC_CS50	63	6.71	23.85	36.89	43.01	45.32	47.74
GPC_CS60	59	6.83	23.68	36.32	45.32	50.86	53.91
GPC_CS70	56	7.23	24.01	37.76	49.86	51.96	54.63
GPC_CS80	50	7.45	23.99	38.43	51.49	53.00	55.76
GPC_CS90	43	9.15	26.14	40.17	57.18	63.21	63.4
GPC_CS100	36	11.83	23.67	38.66	56.29	58.9	59.95

At 28 days, the compressive strength of the HSGPC specimens with 90% copper slag was 33.5 and 62.2% higher for the ambient- and steam-curing conditions, respectively, when compared to the control GPC mix (Figure 6). However, it is worth mentioning that the addition of a large volume of copper slag to 100% did not show any considerable detrimental effects on the compressive strength of the GPC. The compressive strength at 28 days for the GPC specimens with 100% copper slag was 28.5 and 53.4%, respectively, for the ambient- and steam-curing conditions when compared to the control GPC mix. Hence, the GPC specimens with 100% copper slag were considered as the optimum mix and will be used for further evaluation, which includes the effect of the micro silica addition at different dosages.



(**a**)

Figure 6. *Cont.*



(**b**)

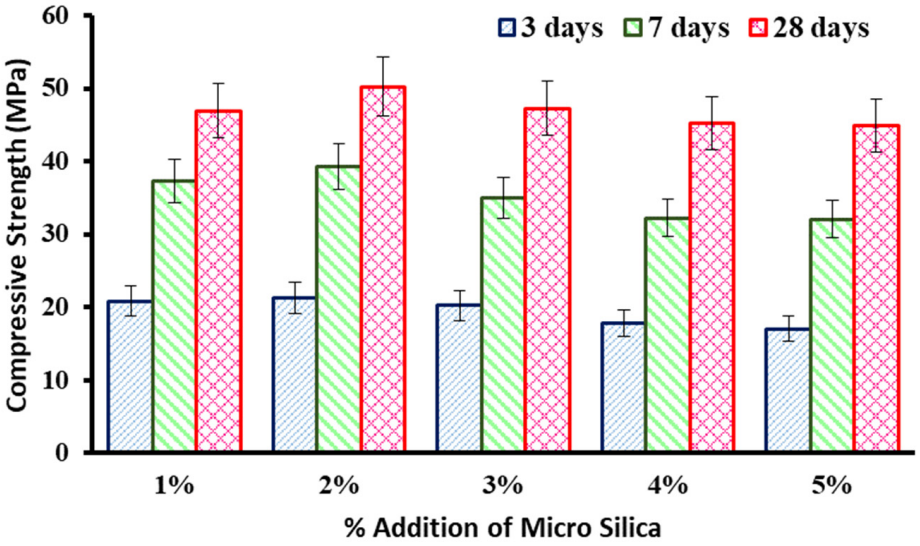
Figure 6. Compressive strength of copper slag-based HSGPC. (**a**) Ambient-cured specimens. (**b**) Steam-cured specimens.

4.2. Evaluation of Optimized Mix

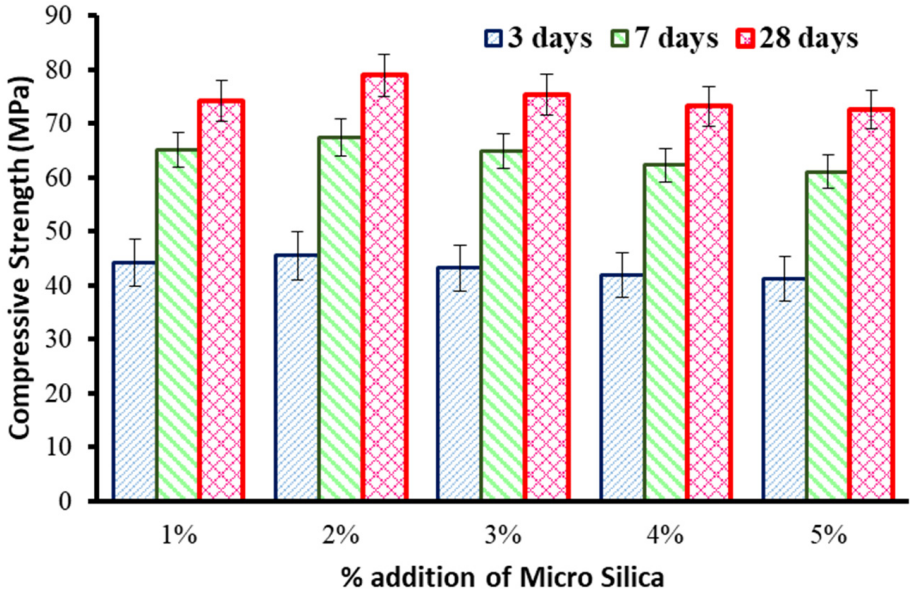
The GPC specimens with 100% copper slag were considered as the optimum mix. This optimized mix was used further with micro silica in the stages of 1% up to a maximum limit of 5%. The effect of the micro silica addition on the performance of the HSGPC specimens was evaluated for the mechanical, durability and microstructural characteristics. The mechanical properties were determined from the compressive strength, splitting tensile strength and ultrasonic pulse velocity tests. The durability properties were determined using the water-absorption and sorptivity tests. The microstructure characterization of the tested GPC samples was performed using the SEM with EDS analyses. The results obtained for the HSGPC specimens with and without micro silica are discussed in the following section.

4.2.1. Compressive Strength

Figure 7 shows the compressive strength of the specimens subjected to ambient- and steam-curing conditions and tested at different ages. From Figure 7, it is clear that the compressive strength of the GPC was found to increase until the addition of 2% micro silica. Micro silica being a pozzolanic material results in a more uniform mix along with the reduction in pore size of the binder paste. However, the addition of more than 2% micro silica in the GPC could result in handling difficulties and the poor distribution of micro silica particles. For the addition of 2% micro silica, the compressive strength of the optimized GPC mix increased by 38.7 and 31.8% for the ambient and steam specimens, respectively. The addition of more than 2% micro silica resulted in a marginal reduction in the compressive strength of the GPC specimens under both ambient- and steam-curing conditions. This is due to the fact that the addition of a higher dosage of micro silica could hinder the geopolymerization process and creates a demand for Na_2O in the alkaline activator [34]. This in turn could result in the reduction in strength. For the addition of 5% micro silica, the increase in compressive strength achieved was 16.1 and 21.1% for the ambient- and steam-curing conditions, respectively.



(**a**)

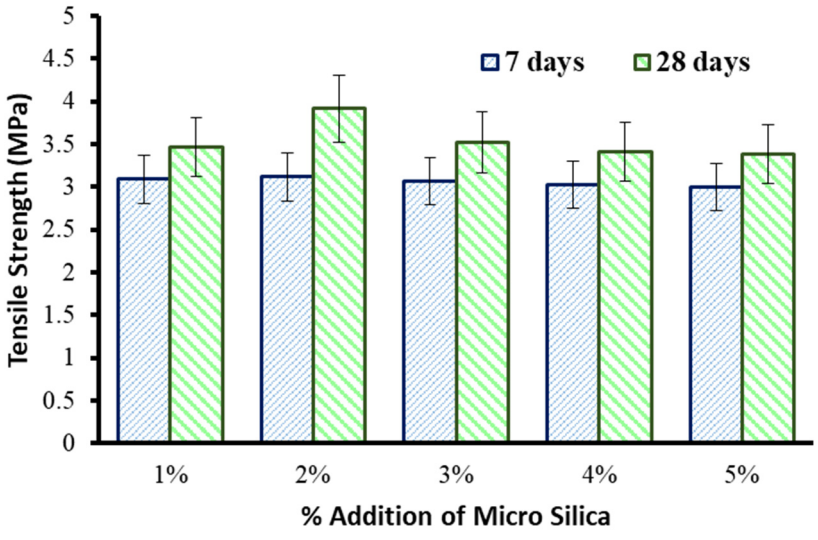


(**b**)

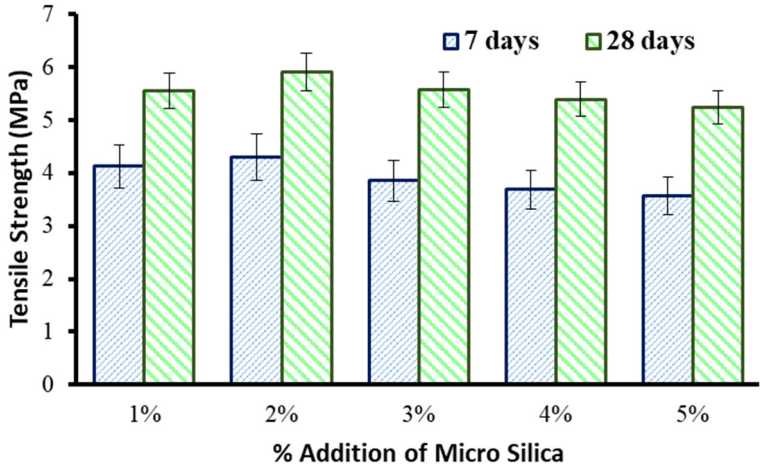
Figure 7. Effect of micro silica on the strength of copper slag-based HSGPC. (**a**) Ambient-cured specimens. (**b**) Steam-cured specimens.

4.2.2. Splitting Tensile Strength

The splitting tensile strength test is conducted in accordance with IS 5816-1999 [77]. Figure 8 shows the tensile strength obtained at ambient- and steam-curing conditions and tested at different ages. Similar to the compressive strength, the values of the splitting tensile strength were found to increase with the increase in micro silica until 2%. For the addition of 2% micro silica, the splitting tensile strength of the optimized GPC mix increased by 12.9 and 6.24% for the ambient and steam specimens, respectively, when compared to the HSGPC with 1% micro silica. Adding a larger dose of micro silica to the alkaline activator might impede the geopolymerization process and increase the need for Na_2O. For the addition of 5% micro silica, the splitting tensile strength of the HSGPC was even less than the specimens with 1% micro silica.



(**a**)



(**b**)

Figure 8. Splitting tensile strength of copper slag-based HSGPC with micro silica. (**a**) Ambient-cured specimens. (**b**) Steam-cured specimens.

4.2.3. Ultrasonic Pulse Velocity

In this study, the ultrasonic pulse velocity (UPV) test, which is a non-destructive evaluation method, was used to understand the quality of high-strength geopolymer concrete. The quality of copper slag-based HSGPC is evaluated in terms of its material homogeneity, the presence of internal flaws and cracks, etc. The ultrasonic pulse velocity test was conducted as specified by Indian Standards [56]. As shown in Figure 9, the test was performed on the high-strength geopolymer concrete cubes of size 100 mm and tested at the 28-day age of the ambient- and steam-curing methods. From the inference of the UPV results, the quality of concrete can be classified under four different categories: (a) Excellent ($v > 4.5$ km/s), (b) Good (3.5 km/s $< v <$ 4.5 km/s), (c) Medium (3.0 km/s $< v <$ 3.5 km/s) and (d) Doubtful ($v <$ 3.0 km/s).

From Figure 10, it can be observed that the velocity for all the cubes was in the range of 3.65 to 3.89 km/s. The pulse velocity obtained for the HSGPC specimens with 100% copper slag (optimized mix) was observed as 3.65 and 3.70 km/s for the ambient-curing and steam-cured specimens, respectively. The quality of the high-strength geopolymer concrete with different copper slag dosages can be brought up under the quality category "Good". However, the addition of micro silica reduced the pulse velocity of the high-strength geopolymer concrete. With the addition of 5% micro silica, the pulse velocity showed a

significant reduction of about 15.7% due to the porous nature of the geopolymer concrete cured under ambient conditions. The value of the pulse velocity for the 5% micro silica specimen was 3.46 km/s and was categorized under the concrete quality of "Medium". From the overall UPV results, it can be concluded that the ambient-cured specimen had a lower velocity due to the presence of gel water formed during the geopolymerization process. This variation in pulse velocity is due to the presence of water in the form of a gel.



Figure 9. UPV Tests measurement on Optimized GPC Mix.

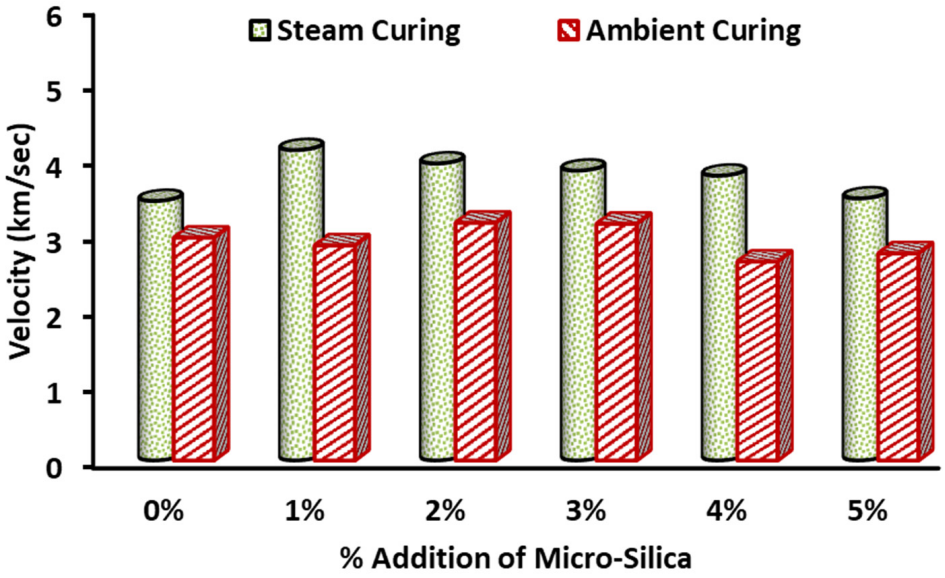


Figure 10. UPV Tests on Optimized GPC Mix.

The dynamic modulus of elasticity can be determined using the ultrasonic pulse velocity and Poisson's ratio using the following relationship

$$E = (v^2 \cdot \rho\ (1 + \mu)\ (1 - 2\mu))/(1 - \mu) \quad (1)$$

where E = dynamic Young's modulus of elasticity in Gpa,

μ = Poisson's ratio,
ρ = density in kg/m^3 and
v = velocity in m/s.

Figure 11 shows the comparison of the dynamic modulus of elasticity and the percentage addition of micro silica. From the results observed, it is clear that the value of E_d reduces with the increase in the micro silica addition similar to the trend of the pulse

velocity. The range of the values of the dynamic elastic modulus for both the ambient- and steam-curing conditions were found to be from 20 to 40 GPa.

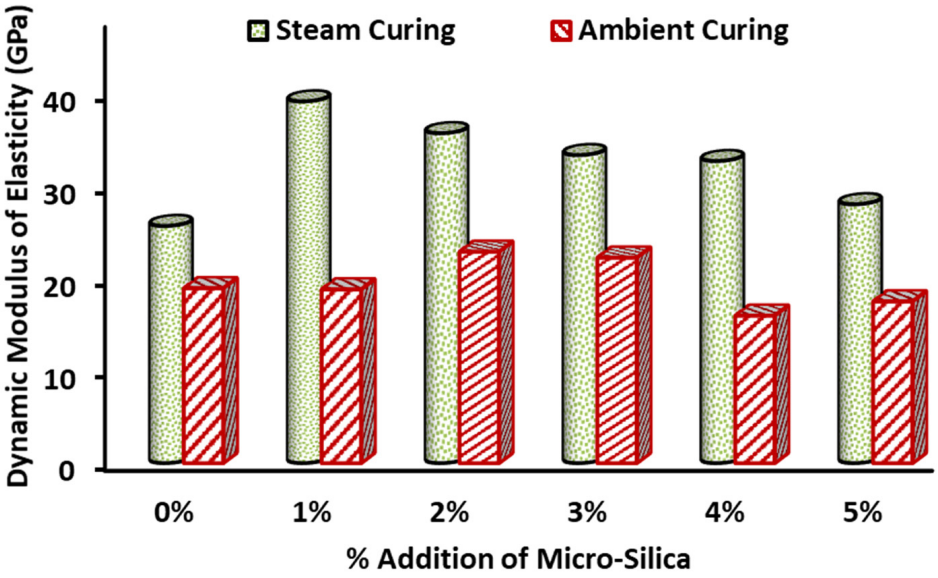


Figure 11. Dynamic modulus of elasticity of the optimized GPC mix.

4.2.4. Water-Absorption Test

The durability of concrete subjected to an aggressive environment mainly depends on the nature of the pore system present in the concrete. ASTM C1585 [78] is used to find out the rate of absorption of water in the concrete. In this study, the water-absorption test for the HSGPC was conducted using the standard cubes (100 mm size) with the addition of micro silica (1%, 2%, 3%, 4% and 5%) and was tested for water absorption at two different time intervals (t = 30 min and 24 h). The initial weight of the sample is taken as W_1 and then the specimen is immersed in water for different time intervals. The final weight of the sample is taken for 30 min as W_2 and also for 24 h as W_3. The percentage absorption of water by each specimen was calculated using Equations (2) and (3).

$$\text{Water Absorption after 30 min (\%)} = [(W_2 - W_1)/W_1] \times 100 \quad (2)$$

$$\text{Water Absorption after 24 h (\%)} = [(W_3 - W_1)/W_1] \times 100 \quad (3)$$

where

W_1 = Dry weight specimen in grams.
W_2 = Weight of sample after immersion in water for 30 min in grams.
W_3 = Weight of sample after immersion in water for 24 h in grams.

The values obtained for different dosages of micro silica are shown in Figure 12. The water absorption of the high-strength geopolymer concrete up to 2% is very low and it increases in further percentages. The water absorption for concrete with higher dosages of micro silica is more when compared to concrete with micro silica less than 2%. Nevertheless, the water absorption values for all the test specimens were found to be less than 1%. Hence, the addition of low levels of micro silica is found desirable as it decreases the total pore volume present in the HSGPC mix and thereby reduces the water absorption [34].

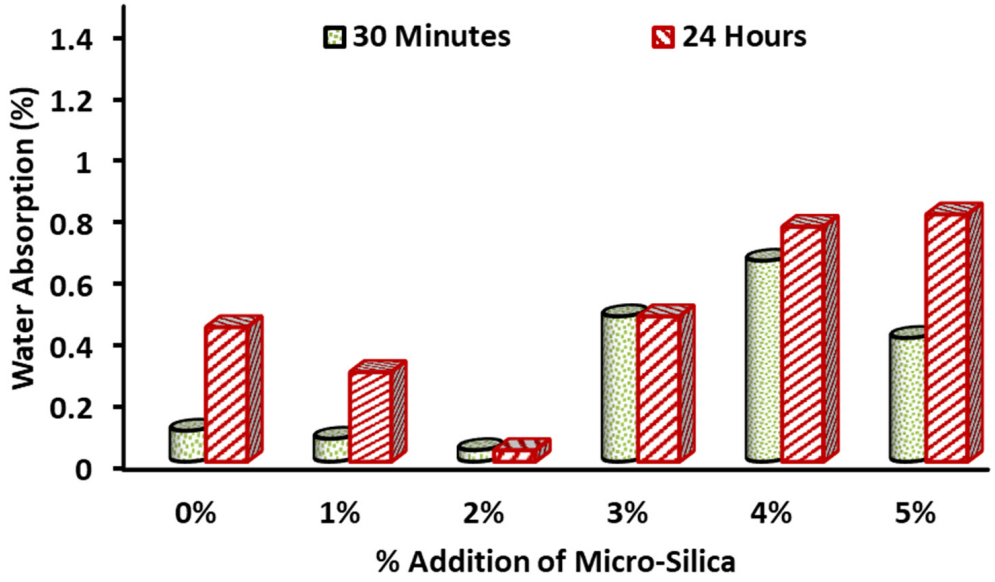


Figure 12. Water-absorption tests on ambient-cured GPC mixes with micro silica.

4.2.5. Sorptivity Tests

The capillary rise of the optimized GPC mixes with different dosages of micro silica is studied using the sorptivity test. Sorptivity can be defined as the property of the porous material that portrays the affinity to absorb and transmit water through the capillary action. The sorptivity test was used for measuring the capillary rise through the test specimen. The cast HSGPC specimens cured for 28 days were immersed in water for 24 h. Then, the specimens were dried at ambient temperature. The cube specimen of size 100 mm was arranged in the water level as per the specifications provided in the ASTM standards [78]. Care should be taken so that the water level is not more than 5 mm above the specimen from the bottom.

For ensuring a unidirectional flow of water through the cube specimen, sealants were used on all sides other than the exposure face. The exterior surface of the test specimen is prevented by sealing with the use of a non-absorbent coating such as paint, epoxy, etc. The specimens are coated with paint on three sides and the bottom surface exposed to water for about 30 min. For every 30 min, the samples were taken out and weighed to determine the water absorption of the specimen. The test is continued for 6 h. As shown in Equations (3) and (4), the cumulative water absorption per unit area of the inflow surface increases as the square root of elapsed time (t). The sorptivity values of all the specimens with micro silica are found to be less than 6 mm (Figure 13). Hence, it can be conferred that the prepared GPC mixes are of good quality and possess excellent durability resistance characteristics.

$$S = I/t^{\frac{1}{2}} \quad (4)$$

$$I = \Delta_w / Ad \quad (5)$$

Δ_w is the difference in weight of dry and immersed specimen = $W_2 - W_1$
A = Surface area of the specimen through which water penetrated and
d = density of fluid used.

where S = Sorptivity (mm), t = Elapsed time in minute,

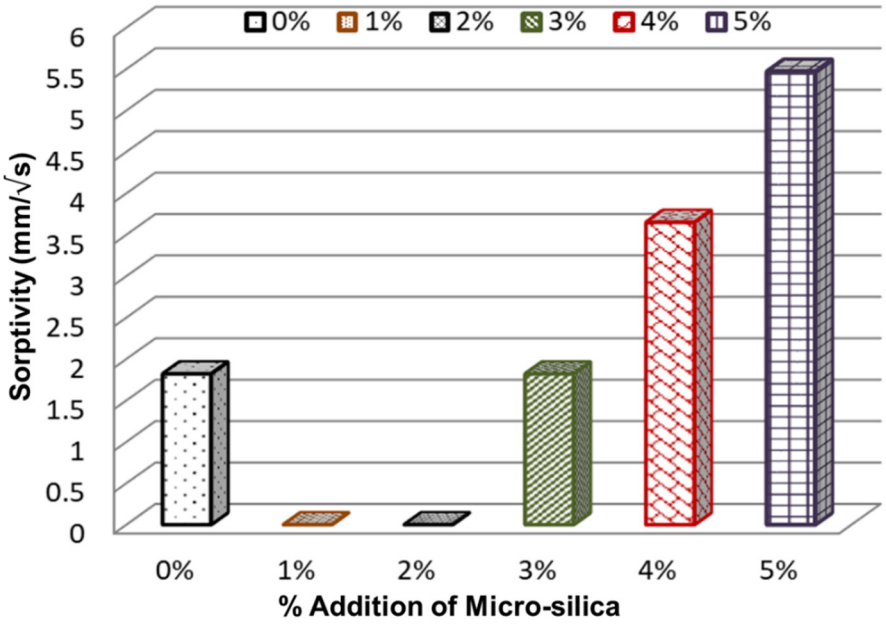


Figure 13. Sorptivity values for ambient-cured GPC mixes with micro silica.

4.3. Microstructural Studies on GPC

The internal microstructure of the high-strength geopolymer concrete (HSGPC) with a high-volume of copper slag and micro silica was studied through the scanning electron microscope (SEM) analyses and the results are presented in Figures 14 and 15. The microstructure analyses were performed to understand the effect of both curing conditions, ambient curing and steam curing. Figure 14a shows the presence of a number of characteristics, such as unreacted fly ash particles, pores, white deposits and the geopolymer binder. At the initial stages, it was observed that a large number of unreacted fly ash particles were present in the specimens. This is due to the fact that the process of ambient curing delayed the process of polymeric gel formation. Numerous micro-cracks and pores were found in the matrix which can be witnessed in Figure 14b. It was due to the insufficient amount of heat that delayed the reaction and also the loss of water in the alkaline solution. Here, the insufficient amount of heat represents that the heat required for taking up the polymerization was not there in the ambient-cured specimens. The loss of water is due to the evaporation as the specimens are left open to the atmosphere for curing. Moreover, the ambient-cured specimen had higher pores which are visible in the SEM image (Figure 14b). These pores in the concrete may be the reason for the absorption of the liquid medium and cause the degradation of strength.

In general, the developed HSGPC mix contains three phases, which include (i) the binder mix, (ii) the aggregate and (iii) the ITZ. Due to the reaction of copper slag with the alkaline solution, a better cementitious binder matrix is developed and gets deposited around the surface of the aggregate. Figure 14c highlights the Interfacial Transition Zone (ITZ) between the aggregate–binder matrix. Also, the binder present shows a number of unreacted cenosphere and plenosphere fly ash particles, which have not reacted with the matrix. These large numbers of unreacted fly ash are present due to the adopted ambient-curing conditions present in the matrix. In addition to these characteristics, a number of white deposits can be witnessed as shown in Figure 14d. However, in the case of the high-strength geopolymer concrete specimens cured with steam method, the microstructure was denser with a fully reacted matrix. However, some unreacted cenosphere fly ash particles were present during the SEM analyses. It is worth mentioning that the unreacted particles were present due to the early age of the concrete during which the testing was performed. Moreover, the presence of a large number of unreacted fly ash particles leads to a decrease in the strength of the developed GPC mixes under ambient-curing conditions. In addition, the matrix also contains a few voids present as shown in Figure 15a. From Figure 15b, it

can be observed that the process of polymerization resulted in the formation of Na-Al-Si-H (sodium Alumino Silicate) gel. Also, observing the interface between the aggregate and binder paste, a strong Interfacial Transition Zone (ITZ) can be observed which results in the high-strength attainment of the developed HSGPC [79,80]. From Figure 15c, a number of micro-cracks could be observed close to the aggregate–binder interface of the matrix. In addition to these characteristics, a number of white deposits could be witnessed. The white deposit present in the scanning electron microscope (SEM) analysis was possibly a reaction component of the silica from the silica fume that reacted with the alkaline activator solution. The N-A-S-H gel formation resulted in the presence of white deposits.

An Electron Dispersive Spectrum (EDS) analysis was performed on the white deposits observed from the SEM analyses to understand the presence of major atomic constituents after reaction. Figure 16 shows the EDS results performed on the white deposits of the steam-cured high-strength geopolymer concrete specimens. From the results, it is clear that the white deposits were composed of sodium, silica, alumina and oxygen as the major constituent elements. This N-A-S-H gel was responsible for the strength development in the HSGPC specimens.

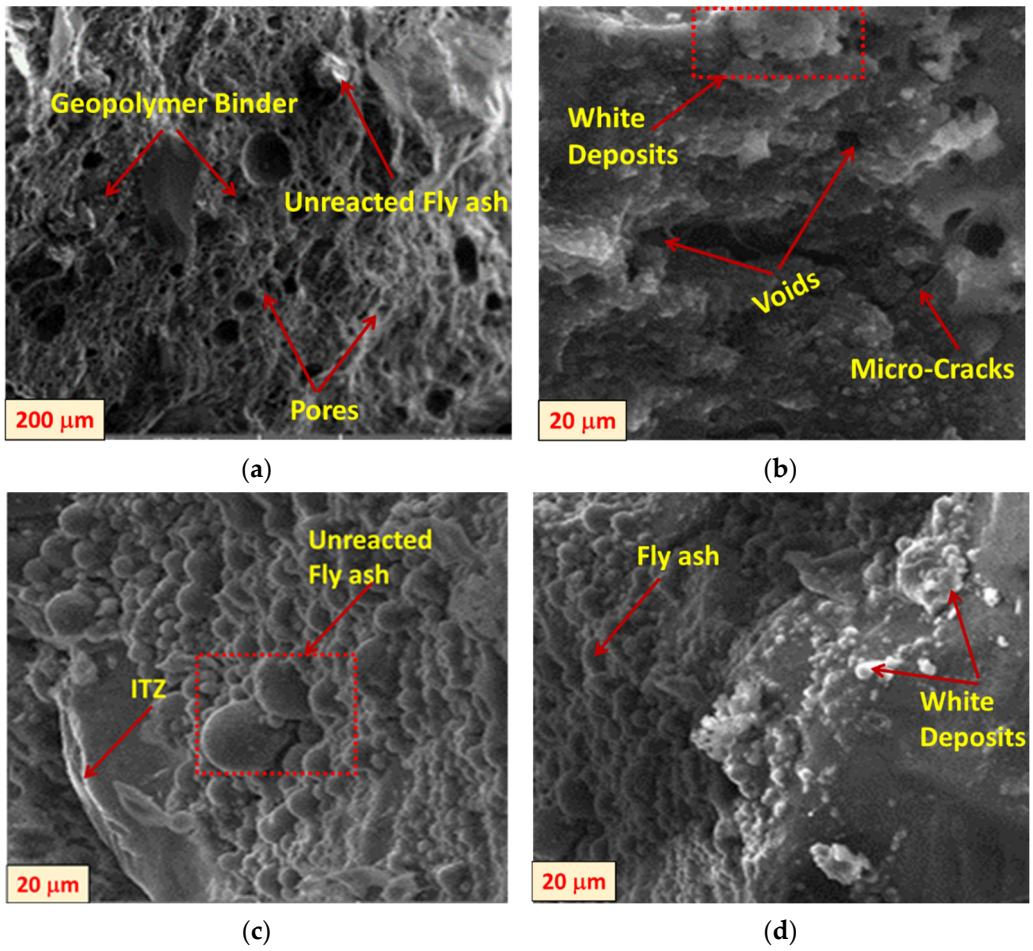


Figure 14. SEM analyses of ambient-cured HSGPC specimens (**a**) appearance of pores (**b**) appearance of voids and micro cracks (**c**) appearance of unreacted fly ash zone and (**d**) appearance of white deposits.

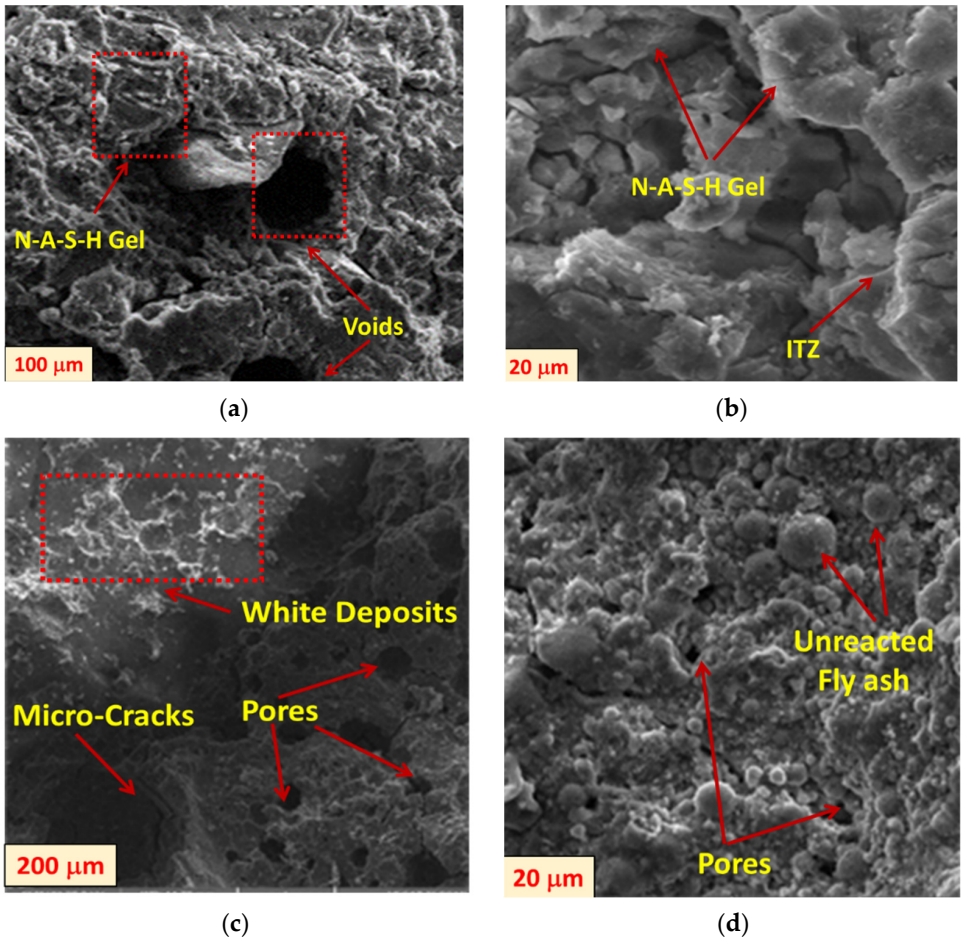


Figure 15. SEM analyses of steam-cured HSGPC specimens (**a**) appearance of voids (**b**) appearance of N-A-S-H gel (**c**) appearance of pores and cracks (**d**) appearance of unreacted flyash and pores.

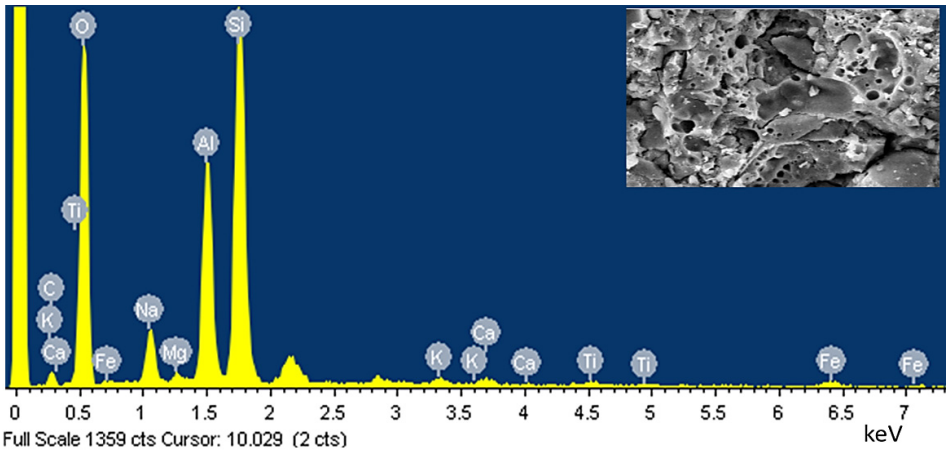


Figure 16. EDS analyses of white deposits in HSGPC specimens.

5. Conclusions

The effect of a micro silica addition on the mechanical, microstructure and durability characteristics of high-strength geopolymer concrete was investigated. In total, 11 initial mixes were prepared by varying the percentage of copper slag up to 100% replacement for river sand. From the mechanical performance of these mixes, an optimum mix with 100% copper slag (GPC_CS100) was selected for further investigation with a silica fume addition. The following major conclusions can be drawn from the results presented in this work:

- The addition of high-volume copper slag resulted in a significant reduction in the workability of the concrete. The reduction in workability could be attributed to the irregular and angular particles present in the copper slag which, when mixed with the HSGPC, resulted in a harsh mixing.
- When the copper slag was used as a fine aggregate for the HSGPC, the compressive strength increased considerably up to 90% sand replacement. For the 100% copper slag replacement, the strength reduction was marginal when compared to the previous mix with 90% replacement.
- From the results of the workability and compressive strength, the optimum mix was selected to be the HSGPC mix with 100% copper slag. This GPC mix when added with micro silica showed an increase in compressive and tensile strength up to the 2% addition. After the 2% addition, the compressive and tensile strength showed a significant reduction.
- From the two curing methods adopted for the HSGPC specimens, the mix cured under the ambient condition showed the least compressive and tensile strength when compared to the steam-cured specimens. For the steam-cured GPC specimen with 100% copper slag, the compressive and tensile strength was 55.1 and 54.8% higher when compared to the tensile strength at the 28-day curing period.
- From the water absorption and sorptivity tests, it can be found that the HSGPC specimens with more than 2% micro silica showed a better performance in terms of low water ingress into the specimen.
- The microstructural analysis of the HSGPC specimens revealed the presence of characteristics, such as white deposits, pores, micro-cracks, Na-Al-Si-H gel and ITZ formation. Moreover, a number of unreacted fly ash particles were witnessed in the case of the ambient-cured GPC specimens due to the insufficient heat generally required to initiate the polymerization reaction.

Author Contributions: Conceptualization, N.A. and M.C.; methodology, N.A. and M.C.; investigation, N.A. and J.M.; validation, N.A., G.M. and N.I.V.; formal analysis, N.A.; data curation, J.M. and G.M.; resources, J.M.; writing—original draft preparation, N.A., M.C., G.M. and N.I.V.; writing—review and editing, N.A., J.M., G.M. and N.I.V.; supervision, M.C.; visualization, M.C.; funding acquisition, G.M. and N.I.V. All authors have read and agreed to the published version of the manuscript.

Funding: The research is partially funded by the Ministry of Science and Higher Education of the Russian Federation as part of the World-class Research Center program: Advanced Digital Technologies (contract No. 075-15-2022-311 dated 20.04.2022).

Institutional Review Board Statement: Not applicable.

Informed Consent Statement: Not applicable.

Data Availability Statement: Not applicable.

Acknowledgments: The first author would like to acknowledge the support and guidance of N. Mahendran, Center for Rural Technology, Gandigram Rural Institute, Dindigul, India.

Conflicts of Interest: The authors declare no conflict of interest.

References

1. Ali, M.B.; Saidur, R.; Hossain, M.S. A review on emission analysis in cement industries. *Renew. Sustain. Energy Rev.* **2011**, *15*, 2252–2261. [CrossRef]
2. Chen, C.; Xu, R.; Tong, D.; Qin, X.; Cheng, J.; Liu, J.; Zheng, B.; Yan, L.; Zhang, Q. A striking growth of CO_2 emissions from the global cement industry driven by new facilities in emerging countries. *Environ. Res. Lett.* **2022**, *17*, 044007. [CrossRef]
3. Gunasekaran, M.; Thangavel, M.; Nemichandran, N.K.; Ravikumar, I.; Glarance, H.J.; Kothandapani, K. Impact response and strength reliability of green high performance fibre reinforced concrete subjected to freeze-thaw cycles in NaCl solution. *Medziagotyra* **2017**, *23*, 384–388. [CrossRef]
4. Berryman, C.; Zhu, J.; Jensen, W.; Tadros, M. High-percentage replacement of cement with fly ash for reinforced concrete pipe. *Cem. Concr. Res.* **2005**, *35*, 1088–1091. [CrossRef]

5. Lo, F.C.; Lee, M.G.; Lo, S.L. Effect of coal ash and rice husk ash partial replacement in ordinary Portland cement on pervious concrete. *Constr. Build. Mater.* **2021**, *286*, 122947. [CrossRef]
6. Chousidis, N.; Rakanta, E.; Ioannou, I.; Batis, G. Mechanical properties and durability performance of reinforced concrete containing fly ash. *Constr. Build. Mater.* **2015**, *101*, 810–817. [CrossRef]
7. Asrani, N.P.; Murali, G.; Parthiban, K.; Surya, K.; Prakash, A.; Rathika, K.; Chandru, U. A feasibility of enhancing the impact resistance of hybrid fibrous geopolymer composites: Experiments and modelling. *Constr. Build. Mater.* **2019**, *203*, 56–68. [CrossRef]
8. Asrani, N.P.; Murali, G.; Abdelgader, H.S.; Parthiban, K.; Haridharan, M.K.; Karthikeyan, K. Investigation on Mode I Fracture Behavior of Hybrid Fiber-Reinforced Geopolymer Composites. *Arabian J. Sci. Eng.* **2019**, *44*, 8545–8555. [CrossRef]
9. Gopalakrishnan, R.; Chinnaraju, K. Durability of ambient cured alumina silicate concrete based on slag/fly ash blends against sulfate environment. *Constr. Build. Mater.* **2019**, *204*, 70–83. [CrossRef]
10. Ibrahim, M.; Azmi, M.; Johari, M.; Maslehuddin, M.; Kalimur, M.; Abiodun, B.; Dafalla, H. Influence of composition and concentration of alkaline activator on the properties of natural-pozzolan based green concrete. *Constr. Build. Mater.* **2019**, *201*, 186–195. [CrossRef]
11. Querol, X.; Plana, F.; Alastuey, A.; Moreno, N.; Izquierdo, M.; Font, O.; Moreno, T.; Diez, S.; Barra, M. Environmental, physical and structural characterisation of geopolymer matrixes synthesised from coal (co-)combustion fly ashes. *J. Hazard. Mater.* **2008**, *154*, 175–183. [CrossRef]
12. Parthiban, K.; Murali, G.; Sreenath, S.; Krishna, A. Effect of Partial Replacement of Ground Granulated Blast Furnace Slag with Sugarcane Bagasse Ash as Source Material in the Production of Geopolymer Concrete. *Mater. Sci.* **2020**, *26*, 477–481.
13. Zhang, J.; Provis, J.L.; Feng, D.; Van Deventer, J.S. Geopolymers for immobilization of Cr^{6+}, Cd^{2+}, and Pb^{2+}. *J. Hazard. Mater.* **2008**, *157*, 587–598. [CrossRef] [PubMed]
14. Abid, S.R.; Murali, G.; Amran, M.; Vatin, N.; Fediuk, R.; Karelina, M. Evaluation of Mode II Fracture Toughness of Hybrid Fibrous Geopolymer Composites. *Materials* **2021**, *14*, 349. [CrossRef]
15. Ryu, G.S.; Lee, Y.B.; Koh, K.T.; Chung, Y.S. The mechanical properties of fly ash-based geopolymer concrete with alkaline activators. *Constr. Build. Mater.* **2013**, *47*, 409–418. [CrossRef]
16. Suksiripattanapong, C.; Horpibulsuk, S.; Chanprasert, P.; Sukmak, P.; Arulrajah, A. Compressive strength development in fly ash geopolymer masonry units manufactured from water treatment sludge. *Constr. Build. Mater.* **2015**, *82*, 20–30. [CrossRef]
17. Sumajouw, D.M.J.; Hardjito, D.; Wallah, S.E.; Rangan, B.V. Fly ash-based geopolymer concrete: Study of slender reinforced columns. *J. Mater. Sci.* **2007**, *42*, 3124–3130. [CrossRef]
18. Ismail, I.; Bernal, S.A.; Provis, J.L.; San Nicolas, R.; Brice, D.G.; Kilcullen, A.R.; Hamdan, S.; Van Deventer, J.S.J. Influence of fly ash on the water and chloride permeability of alkali-activated slag mortars and concretes. *Constr. Build. Mater.* **2013**, *48*, 1187–1201. [CrossRef]
19. Peng, Z.; Vance, K.; Dakhane, A.; Marzke, R.; Neithalath, N. Microstructural and 29Si MAS NMR spectroscopic evaluations of alkali cationic effects on fly ash activation. *Cem. Concr. Compos.* **2014**, *57*, 34–43. [CrossRef]
20. Das, S.; Yang, P.; Singh, S.S.; Mertens, J.C.E.; Xiao, X.; Chawla, N.; Neithalath, N. Effective properties of a fly ash geopolymer: Synergistic application of X-ray synchrotron tomography, nanoindentation, and homogenization models. *Cem. Concr. Res.* **2015**, *78*, 252–262. [CrossRef]
21. Cyr, M.; Pouhet, R. Carbonation in the pore solution of metakaolin-based geopolymer. *Cem. Concr. Res.* **2016**, *88*, 227–235. [CrossRef]
22. Gharzouni, A.; Joussein, E.; Samet, B.; Baklouti, S.; Rossignol, S. Effect of the reactivity of alkaline solution and metakaolin on geopolymer formation. *J. Non-Cryst. Solids* **2015**, *410*, 127–134. [CrossRef]
23. Kuenzel, C.; Li, L.; Vandeperre, L.; Boccaccini, A.R.; Cheeseman, C.R. Influence of sand on the mechanical properties of metakaolin geopolymers. *Constr. Build. Mater.* **2014**, *66*, 442–446. [CrossRef]
24. Karthik, S.; Mohan, K.S.R.; Murali, G. Investigations on the response of novellayered geopolymer fibrous concrete to drop weight impact. *Buildings* **2022**, *12*, 100. [CrossRef]
25. Cheng, H.; Lin, K.L.; Cui, R.; Hwang, C.L.; Cheng, T.W.; Chang, Y.M. Effect of solid-to-liquid ratios on the properties of waste catalyst-metakaolin based geopolymers. *Constr. Build. Mater.* **2015**, *88*, 74–83. [CrossRef]
26. Shah, A. Optimum Utilization of GGBS in Fly Ash based Geopolymer Concrete. *Kalpa Publ. Civ. Eng.* **2018**, *1*, 431–440. [CrossRef]
27. Das, S.K.; Mustakim, S.M.; Adesina, A.; Mishra, J.; Alomayri, T.S.; Assaedi, H.S.; Kaze, C.R. Fresh, strength and microstructure properties of geopolymer concrete incorporating lime and silica fume as replacement of fly ash. *J. Build. Eng.* **2020**, *32*, 101780. [CrossRef]
28. Bajpai, R.; Choudhary, K.; Srivastava, A.; Sangwan, K.S.; Singh, M. Environmental impact assessment of fly ash and silica fume based geopolymer concrete. *J. Clean. Prod.* **2020**, *254*, 120147. [CrossRef]
29. Preethi, P.; Sintha, N.; Prithivi Raj, M.; Tamilarasan, K.; Vinith, R. Exploration on geopolymer concrete using GGBS and silica fume. *Mater. Today Proc.* **2020**. [CrossRef]
30. Krishna Rao, A.; Rupesh Kumar, D. Comparative study on the behaviour of GPC using silica fume and fly ash with GGBS exposed to elevated temperature and ambient curing conditions. *Mater. Today Proc.* **2020**, *27*, 1833–1837. [CrossRef]
31. Shakouri, S.; Bayer, Ö.; Erdoğan, S.T. Development of silica fume-based geopolymer foams. *Constr. Build. Mater.* **2020**, *260*, 120442. [CrossRef]

32. Wang, Y.C.; Zhao, J.P.; Chen, J. Effect of polydimethylsiloxane viscosity on silica fume-based geopolymer hybrid coating for flame-retarding plywood. *Constr. Build. Mater.* **2020**, *239*, 117814. [CrossRef]
33. Adak, D.; Sarkar, M.; Mandal, S. Structural performance of nano-silica modified fly-ash based geopolymer concrete. *Constr. Build. Mater.* **2017**, *135*, 430–439. [CrossRef]
34. Okoye, F.N.; Durgaprasad, J.; Singh, N.B. Effect of silica fume on the mechanical properties of fly ash based-geopolymer concrete. *Ceram. Int.* **2016**, *42*, 3000–3006. [CrossRef]
35. Agrawal, U.S.; Wanjari, S.P.; Naresh, D.N. Impact of replacement of natural river sand with geopolymer fly ash sand on hardened properties of concrete. *Constr. Build. Mater.* **2019**, *209*, 499–507. [CrossRef]
36. Saviour, N.M. Naveen Saviour Environmental Impact of Soil and Sand Mining: A Review. *Int. J. Sci. Environ.* **2012**, *1*, 125–134.
37. Aldemir, A.; Akduman, S.; Kocaer, O.; Aktepe, R.; Sahmaran, M.; Yildirim, G.; Almahmood, H.; Ashour, A. Shear behaviour of reinforced construction and demolition waste-based geopolymer concrete beams. *J. Build. Eng.* **2022**, *47*, 103861. [CrossRef]
38. Mithun, B.M.; Narasimhan, M.C. Performance of alkali activated slag concrete mixes incorporating copper slag as fine aggregate. *J. Clean. Prod.* **2016**, *112*, 837–844. [CrossRef]
39. Gomes Silveira, N.C.; Figueiredo Martins, M.L.; da Bezerra, A.C.S.; da Silva Araújo, F.G. Ecological geopolymer produced with a ternary system of red mud, glass waste, and Portland cement. *Clean. Eng. Technol.* **2022**, *6*, 100379. [CrossRef]
40. Fořt, J.; Novotný, R.; Vejmelková, E.; Trník, A.; Rovnaníková, P.; Keppert, M.; Pommer, V.; Černý, R. Characterization of geopolymers prepared using powdered brick. *J. Mater. Res. Technol.* **2019**, *8*, 6253–6261. [CrossRef]
41. Guo, X.; Yang, J. Intrinsic properties and micro-crack characteristics of ultra-high toughness fly ash/steel slag based geopolymer. *Constr. Build. Mater.* **2020**, *230*, 116965. [CrossRef]
42. Gong, W.; Chen, Q.; Miao, J. Bond behaviors between copper slag concrete and corroded steel bar after exposure to high temperature. *J. Build. Eng.* **2021**, *44*, 103312. [CrossRef]
43. Resende, C.; Cachim, P.; Bastos, A.M. Copper slag mortar properties. *Mater. Sci. Forum* **2008**, *587–588*, 862–866. [CrossRef]
44. Singh, J.; Singh, S.P. Development of Alkali-activated Cementitious Material using Copper Slag. *Constr. Build. Mater.* **2019**, *211*, 73–79. [CrossRef]
45. Madheswaran, C.K.; Ambily, P.S.; Dattatreya, J.K.; Rajamane, N.P. Studies on use of Copper Slag as Replacement Material for River Sand in Building Constructions. *J. Inst. Eng. Ser. A* **2014**, *95*, 169–177. [CrossRef]
46. Ambily, P.S.; Umarani, C.; Ravisankar, K.; Prem, P.R.; Bharatkumar, B.H.; Iyer, N.R. Studies on ultra high performance concrete incorporating copper slag as fine aggregate. *Constr. Build. Mater.* **2015**, *77*, 233–240. [CrossRef]
47. Sudarvizhi, M.; Ilangovan, R. Performance of Copper slag and ferrous slag as partial replacement of sand in Concrete. *Int. J. Civ.* **2011**, *1*, 918–927.
48. Brindha, D.; Nagan, S. Durability studies on copper slag admixed concrete. *Asian J. Civ. Eng.* **2011**, *12*, 563–578.
49. Palani, T.; Jaya, K.P.; Muthumani, K. Studies on copper slag substitution for sand in high strength concrete. *J. Struct. Eng.* **2014**, *41*, 293–306.
50. Al-Jabri, K.S.; Al-Saidy, A.H.; Taha, R. Effect of copper slag as a fine aggregate on the properties of cement mortars and concrete. *Constr. Build. Mater.* **2011**, *25*, 933–938. [CrossRef]
51. Sharma, R.; Khan, R.A. Sustainable use of copper slag in self-compacting concrete containing supplementary cementitious materials. *J. Clean. Prod.* **2017**, *151*, 179–192. [CrossRef]
52. Sivasakthi, M.; Jeyalakshmi, R.; Rajamane, N.P. Fly ash geopolymer mortar: Impact of the substitution of river sand by copper slag as a fine aggregate on its thermal resistance properties. *J. Clean. Prod.* **2021**, *279*, 123766. [CrossRef]
53. Bell, J.L.; Sarin, P.; Provis, J.L.; Haggerty, R.P.; Driemeyer, P.E.; Chupas, P.J.; Van Deventer, J.S.; Kriven, W.M. Atomic structure of a cesium aluminosilicate geopolymer: A pair distribution function study. *Chem. Mater.* **2008**, *20*, 4768–4776. [CrossRef]
54. Aguirre-guerrero, A.M.; Robayo-salazar, R.A.; De Gutiérrez, R.M. Applied Clay Science A novel geopolymer application: Coatings to protect reinforced concrete against corrosion. *Appl. Clay Sci.* **2017**, *135*, 437–446. [CrossRef]
55. Guo, X.; Hu, W.; Shi, H. Microstructure and self-solidification/stabilization (S/S) of heavy metals of nano-modified CFA—MSWIFA composite geopolymers. *Constr. Build. Mater.* **2014**, *56*, 81–86. [CrossRef]
56. Kim, B.; Lee, J.; Kang, J.; Um, W. Development of geopolymer waste form for immobilization of radioactive borate waste. *J. Hazard. Mater.* **2021**, *419*, 126402. [CrossRef]
57. Mahmed, N.; Nor, S.; Zailan, S.; Al-bakri, M.M. Influence of TiO_2 nanoparticles (wt %) onto the physical and mechanical properties of the TiO_2-geopolymer paste. In *IOP Conference Series: Materials Science and Engineering*; IOP Publishing: Bristol, UK, 2020. [CrossRef]
58. Nasvi, M.C.M.; Rathnaweera, T.D.; Padmanabhan, E. Geopolymer as well cement and its mechanical integrity under deep down-hole stress conditions: Application for carbon capture and storage wells. *Geomech. Geophys. Geo-Energy Geo-Resour.* **2016**, *2*, 245–256. [CrossRef]
59. Wu, Y.; Lu, B.; Yi, Z.; Du, F.; Zhang, Y. *The Properties and Latest Application of The Properties and Latest Application of Geopolymers*; Elsevier: Amsterdam, The Netherlands, 2019. [CrossRef]
60. Zhang, Z.; Wang, K.; Mo, B.; Li, X.; Cui, X. Preparation and characterization of a reflective and heat insulative coating based on geopolymers. *Energy Build.* **2015**, *87*, 220–225. [CrossRef]
61. Provis, J.L. Immobilisation of toxic wastes in geopolymers. In *Geopolymers: Structures, Processing, Properties and Industrial Applications*; Woodhead Publishing: Cambridge, UK, 2009; pp. 421–440. [CrossRef]

62. ASTM. *Standard Specification for Coal Fly-Ash and Raw or Calcined Natural Pozzolan for Use*; Annual Book of ASTM Standards: Philadelphia, PA, USA, 2010; pp. 3–6.
63. Wang, J.; Erdenbold, U. A study on reduction of copper smelting slag by carbon for recycling into metal values and cement raw material. *Sustainability* **2020**, *12*, 1421. [CrossRef]
64. Tixier, R.; Devaguptapu, R.; Mobasher, B. The Effect of Copper Slag on the Hydration and Mechanical Properties of Cementitious Mixtures. *Cem. Concr. Res.* **1997**, *27*, 1569–1580. [CrossRef]
65. Moeini, M.A.; Bagheri, M.; Joshaghani, A.; Ramezanianpour, A.A.; Moodi, F. Feasibility of Alkali-Activated Slag Paste as Injection Material for Rehabilitation of Concrete Structures. *J. Mater. Civ. Eng.* **2018**, *30*, 04018252. [CrossRef]
66. Maddalena, R.; Hall, C.; Hamilton, A. Effect of silica particle size on the formation of calcium silicate hydrate [C-SH] using thermal analysis. *Thermochim. Acta.* **2019**, *672*, 142–149. [CrossRef]
67. Najimi, M.; Sobhani, J.; Pourkhorshidi, A.R. Durability of copper slag contained concrete exposed to sulfate attack. *Constr. Build. Mater.* **2011**, *25*, 1895–1905. [CrossRef]
68. *IS 383*; Coarse and Fine Aggregate for Concrete—Specification. Bureau of Indian Standards: New Delhi, India, 2016; pp. 1–30.
69. Rajamane, J.R. *Quantities of Sodium Hydroxide Solids and Water to Prepare Sodium Hydroxide Solution of Given Molarity for Geopolymer Concrete Mixes*; ICI Technical Paper; SRM University: Kattankulathur, India, 2014; pp. 4–9.
70. Pavithra, P.; Reddy, M.S.; Dinakar, P.; Rao, B.H.; Satpathy, B.H.; Mohanty, A.N. A mix design procedure for geopolymer concrete with fly-ash. *J. Clean. Prod.* **2016**, *133*, 117–125. [CrossRef]
71. Adam, A.A.; Horianto, X.X.X. The effect of temperature and duration of curing on the strength of fly-ash based geopolymer mortar. *Procedia Eng.* **2014**, *95*, 410–414. [CrossRef]
72. Nuruddin, M.F.; Demie, S.; Ahmed, M.F.; Shafiq, N. Effect of superplasticizer and NaOH molarity on workability, compressive strength and microstructure properties of self-compacting geopolymer concrete. *World Acad. Sci. Eng. Technol.* **2011**, *51*, 907–914.
73. Jithendra, C.; Elavenil, S. Role of superplasticizer on GGBS based Geopolymer concrete under ambient curing. *Mater. Today Proc.* **2019**, *18*, 148–154. [CrossRef]
74. Lăzărescu, A.V.; Szilagyi, H.; Baeră, C.; Ioani, A. The Effect of Alkaline Activator Ratio on the Compressive Strength of Fly-ash-based Geopolymer Paste. In *IOP Conference Series: Materials Science and Engineering*; IOP Publishing: Bristol, UK, 2017; Volume 209.
75. Oyebisi, S.; Ede, A.; Olutoge, F.; Igba, T.; Oluwafemi, J. Effects of rest period on the strength performance of geopolymer concrete. In *IOP Conference Series: Materials Science and Engineering*; IOP Publishing: Bristol, UK, 2019; Volume 640.
76. *IS 516*; Method of Tests for Strength of Concrete. Bureau of Indian Standards: New Delhi, India, 1959; pp. 1–30.
77. *IS 5816*; Splitting Tensile Strength of Concrete—Method of Test. Bureau of Indian Standards: New Delhi, India, 1999; pp. 1–14.
78. *ASTM C-1585-04*; Standard Test Method for Measurement of Rate of Absorption of Water by Hydraulic—Cement Concretes. American Society for Testing and Materials: West Conshohocken, PA, USA, 2020; pp. 1–6.
79. Kai, M.F.; Dai, J.G. Understanding geopolymer binder-aggregate interfacial characteristics at molecular level. *Cem. Concr. Res.* **2021**, *149*, 106582. [CrossRef]
80. Ren, X.; Zhang, L. Experimental study of interfacial transition zones between geopolymer binder and recycled aggregate. *Constr. Build. Mater.* **2018**, *167*, 749–756. [CrossRef]